Polymer Research Laboratory, BASF Aktiengesellschaft,
Ludwigshafen/Rhein, Federal Republic of Germany

Laboratory tests of ELASTOL (Oil Spill Combat Agent)

H.M. Laun and R. Hingmann

I. Introduction

ELASTOL* is manufactured in the form of a white powder with particle sizes between 100 µm and 1000 µm (Fig.1).

Fig.1: The powder form of ELASTOL simplifies application.

* ELASTOL is a trademark of General Technology Applications Inc. and BASF Aktiengesellschaft

The powder contains about 50% by weight of Polyisobutylene (PIB) of extremely high molar mass ($M_W \approx 6 \cdot 10^6$ g/mol). PIB is a non-toxic polymer that only consists of carbon and hydrogen atoms. The chemical composition is

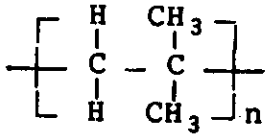

Fully extended the polymer chain would reach a length of about 17 µm. Granules of polymeric material are coated with water-insoluble $Ca_5(PO_4)_3OH$ salt in order to obtain an easily spreadable, non-agglomerating powder. Only the PIB-component is soluble in oil. When dissolved the macromolecules give rise to a distinct viscoelasticity as well as a drastic increase in the elongational viscosity of the solution even at PIB concentrations of only a few hundred ppm.

These properties make ELASTOL a very interesting oil spill treating agent [1]. The performance of skimmers is improved, the resistance to spreading and break-up is greater, and the speed of collecting barriers can be increased.

In this work we report laboratory tests with ELASTOL applied to different oils at various concentrations. The intention is on one hand to give quantitative data on both the rheological properties of the ELASTOL treated oils and on the dissolving kinetics of the powder. On the other hand we try to illustrate the basic mechanisms that are responsible for the observed properties of the solution. These properties are mainly due to the stretching and orientation of the dissolved polymer chain. These are purely physical effects which work independently of possibly present chemically active additives.

In Table 1 the fractionated oils and crude oils used in this investigation are listed. η_0 is the zero shear rate viscosity of the oils at 25 °C.

Table 1: List of oils used in this investigation and their zero shear rate viscosities η_0 at 25 °C.

fractionated oils	η_0 [mPa·s]
Petroleum	1.42
Heizöl	3.65
Dieselöl (Columbia Diesel)	6.9
Spindelöl	7.0
Getriebeöl/Petroleum 1/1 (mixture)	10.5
Trafoöl	13.0
Marcol 82 (Exxon)	21.6
Feinmechanikeröl	34.3
Vakuumpumpenöl	190
Getriebeöl	713

crude oils	η_0 [mPa·s]
Quaibo	4.6
Arabmed	18.0
Venezolana/Quaibo 61/39 (mixture)	70.0

II. Rheological properties of ELASTOL oil solutions

1. Dependence of the solution viscosity on the type of oil

The oils listed in Table 1 were treated with both 2 000 ppm and 10 000 ppm (0.2 and 1% by weight) ELASTOL. The solutions were produced by rolling the powder-oil mixtures in closed glass bottles at about 120 rpm and 23 °C for a time period of 30 to 70 hours.

The viscosity of the resulting solutions was determined by means of a high precision Couette Rheometer (Contraves LS 30). This instrument can measure shear stresses ranging from about $3 \cdot 10^{-4}$ Pa to 4 Pa in a shear rate range between $3 \cdot 10^{-3}$ s^{-1} and 100 s^{-1}.

In general the PIB solutions are non-Newtonian, viz. the viscosity of the fluid is dependent on the shear rate. In our measurements, therefore, shear rates small enough to get the constant viscosity η_s at the limit of small shear rates (zero shear rate viscosity) were used. The data are listed in Table 2.

Table 2: Viscosity increase due to ELASTOL (dissolved by rolling) in various oils for powder concentrations of 2 000 and 10 000 ppm. Viscosities were measured at 25 °C.

oil		c = 2 000 ppm		c = 10 000 ppm	
	η_0 [mPa·s]	η_s [mPa·s]	η_r	η_s [mPa·s]	η_r
Petroleum	1.42	3.02	2.13	23.3	16.3
Heizöl	3.65	7.54	2.07	52.3	14.3
Spindelöl	7.0	15.1	2.16	97.1	13.9
Getriebeöl/ Petroleum 1/1	10.45	17.1	1.64	83.4	7.9
Trafoöl	13.0	22.7	1.75	122.6	9.4
Marcol 82	21.6	36.1	1.67	178	8.2
Vakuumpumpenöl	190	238.4	1.25	908	4.8
Getriebeöl	713	845.6	1.19	1656	2.3
Quaibo	4.6	8.5	1.85	46.2	10.0
Arabmed	18.0	24.0	1.33	74.6	4.1
Venezolana/ Quaibo 61/39	70	83.7	1.20	241	3.4

In the case of the most viscous oils (Vakuumpumpenöl, Getriebeöl) and a powder concentration of 10 000 ppm the PIB could not entirely be dissolved even after a rolling time of > 70 h. For these two samples the η_s-values only represent lower limits of the viscosity of a homogeneous solution.

The relative viscosities η_r

$$\eta_r = \eta_s/\eta_0 \qquad (1)$$

also listed in Table 2 are the ratios of solution viscosity and oil viscosity. η_r increases with increasing powder concentration. It is also seen that the relative viscosity increase due to ELASTOL becomes smaller with increasing viscosity of the oil. For 1% concentration we get a relative viscosity of 16.3 for Petroleum, compared to 4.8 for Vakuumpumpenöl.

In Figure 2 and Figure 3 the relative viscosities are plotted versus the logarithm of the oil viscosity for 2 000 ppm and 10 000 ppm powder, respectively. It is interesting to note that for the

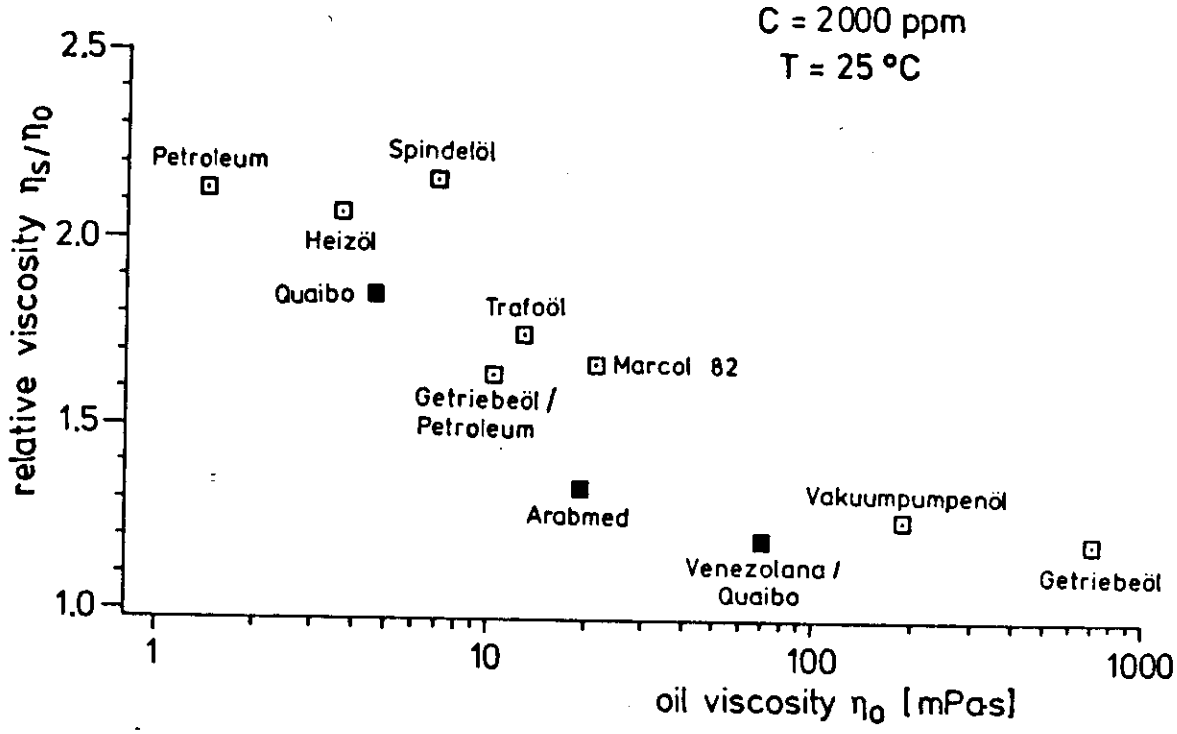

Fig.2: Relative viscosities η_r for various oils as obtained after rolling powder oil mixtures with an ELASTOL concentration of 2 000 ppm at 25 °C. Open symbols represent fractionated oils, full symbols crude oils.

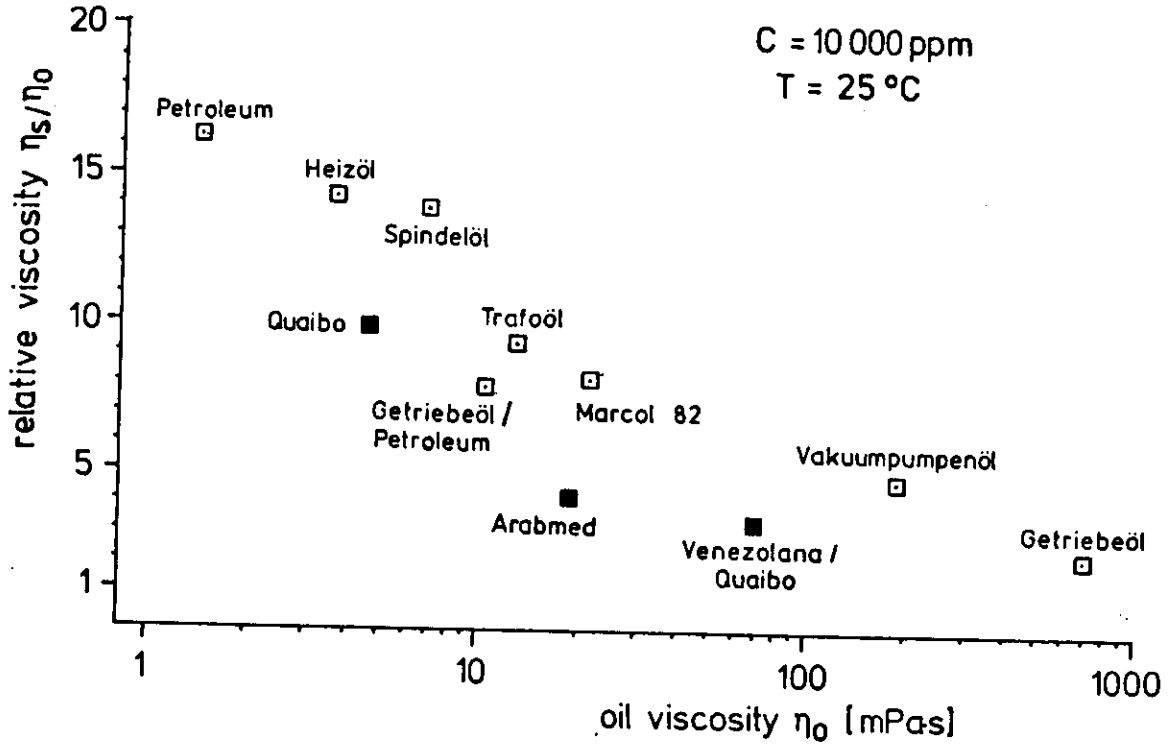

Fig.3: Same as Fig.1 for an ELASTOL concentration of 10 000 ppm.

1/1 mixture of Petroleum and Getriebeöl as well as for the crude oils, the relative viscosities are significantly smaller compared to fractionated oils of similar viscosity. A possible explanation for the observed effect might be the reduction of the coil extension in the oil mixtures due to changes in the average polymer-solvent interaction.

2. Dependence of solution viscosity on powder concentration

Zero shear rate viscosities η_s were measured on solutions in Petroleum and Heizöl at various concentrations. For this purpose base solutions having 6 000 ppm ELASTOL were prepared and subsequently diluted by adding solvent. The resulting data are shown in Figure 4.

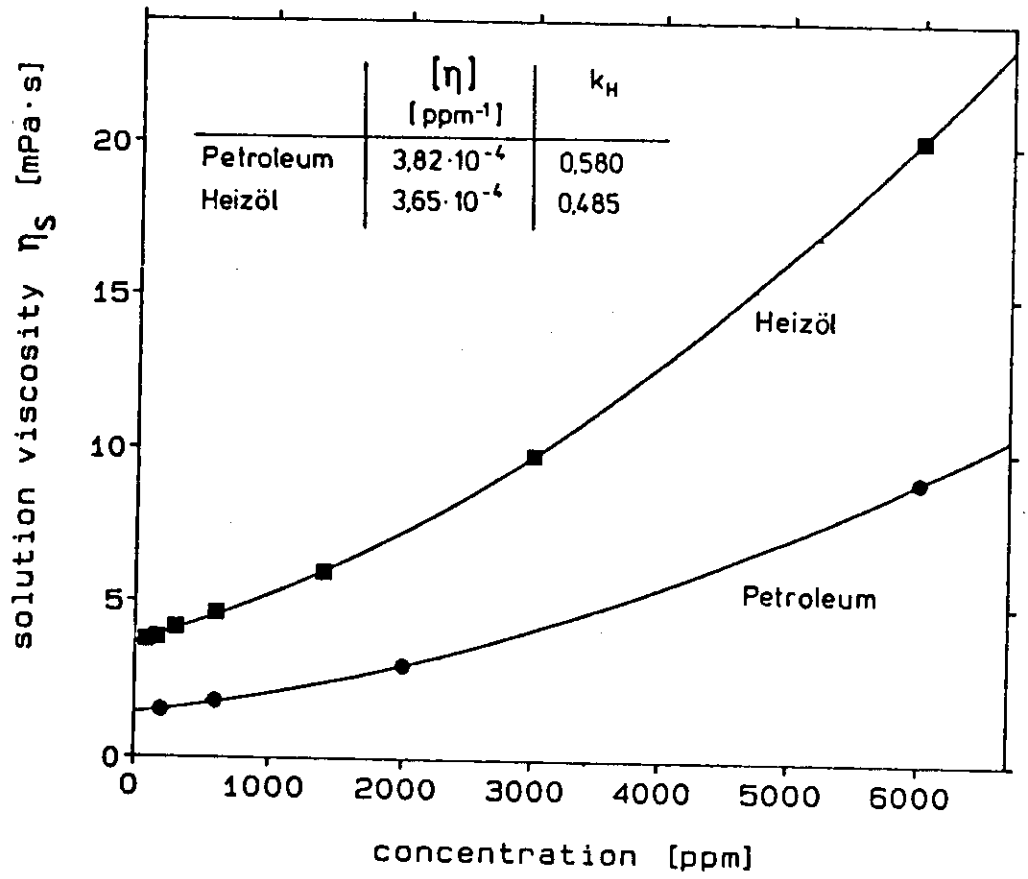

Fig.4: Solution viscosity η_S versus ELASTOL concentration for Petroleum and Heizöl. Full lines represent the fit by the Huggins equation (see text) using the parameters given in the inserted table.

The viscosity of the solutions increases stronger than proportional to the powder concentration in the range tested. The experimental results are nicely described by a polynomial of order 2 (full lines) as proposed by Huggins [2]:

$$\eta_S = \eta_0 \, (1 + [\eta]c + k_H \, [\eta]^2 \, c^2) \quad , \qquad (2)$$

$[\eta]$ being the intrinsic viscosity and k_H the Huggins constant. The values determined by a best fit to the data points are given in the diagram.

3. Viscoelasticity of ELASTOL solutions

The solutions were submitted to small amplitude oscillatory shear in a rotational rheometer using bi-cone geometry. The apparatus is schematically depicted in Figure 5. A gap angle of $\alpha = 3.8°$ and angular frequencies $\omega = 2\pi f$ (f frequency of the oscillation) in the range of 0.2 to 18 s^{-1} were used. The shear amplitude was $\hat{\gamma} = 0.5$.

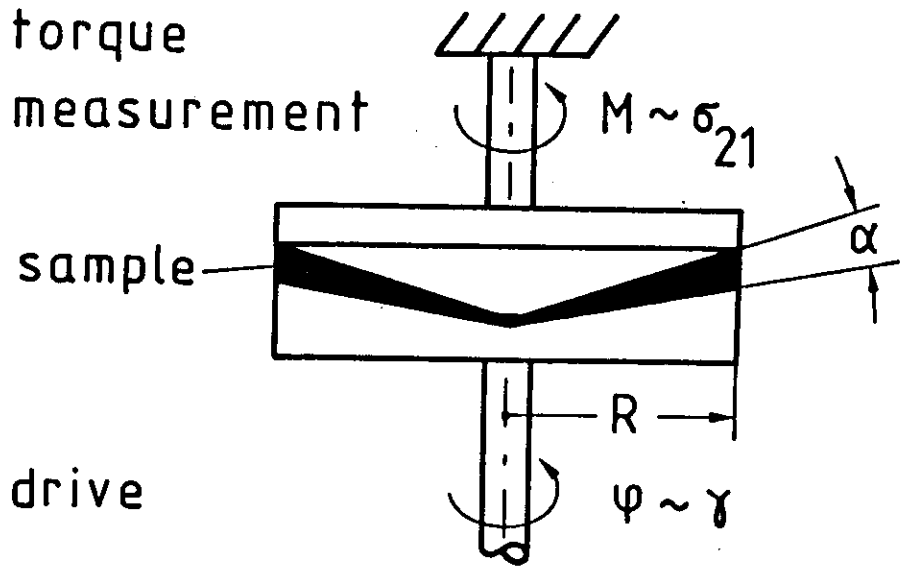

Fig.5: Schematic drawing of the bi-cone geometry used for small amplitude oscillatory shear.

The resulting shear stress σ_{21} is oscillating at the same frequency but is phase shifted compared to the shear strain γ [3] (see Fig.6). It can be decomposed into Sine and Cosine components by means of a frequency response analyzer.

The direct output of the measurements are the storage modulus G' and the loss modulus G" as functions of the angular frequency ω. In our experiments the contribution of inertia forces to G' has been corrected for analytically.

shear strain γ:

$$\gamma = \hat{\gamma} \sin \omega t$$

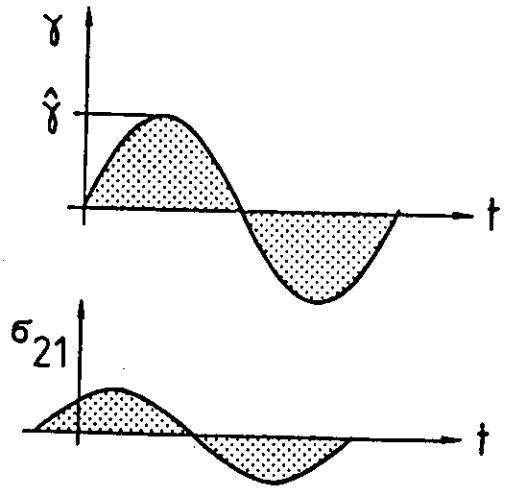

shear stress σ_{21}:

$$\sigma_{21} = \hat{\gamma} [G' \sin \omega t + G'' \cos \omega t]$$

G'': loss modulus

G': storage modulus

Fig.6: Decomposition of the phase shifted oscillating shear stress into two components yields the storage modulus G' and the loss modulus G".

In general the response of solutions to oscillatory shear can be described by an elastic spring G' and a dashpot $\eta = G''/\omega$ arranged in parallel [3] (Fig.7). A purely viscous fluid of viscosity η can be represented by the dashpot alone and the shear stress is proportional to the shear rate $\dot{\gamma}$ which yields a phase shift of 90 degrees between stress and strain. The dissipated energy per cycle is proportional to the loss modulus G". An elastic material (e.g. ideal rubber) can be represented by the spring. Here the stress is proportional to the strain (no phase shift). The storage modulus G' represents the spring constant and is proportional to the stored energy per cycle. A viscoelastic material has both components. The quantity G'/G" is equal to the ratio of stored and dissipated energy.

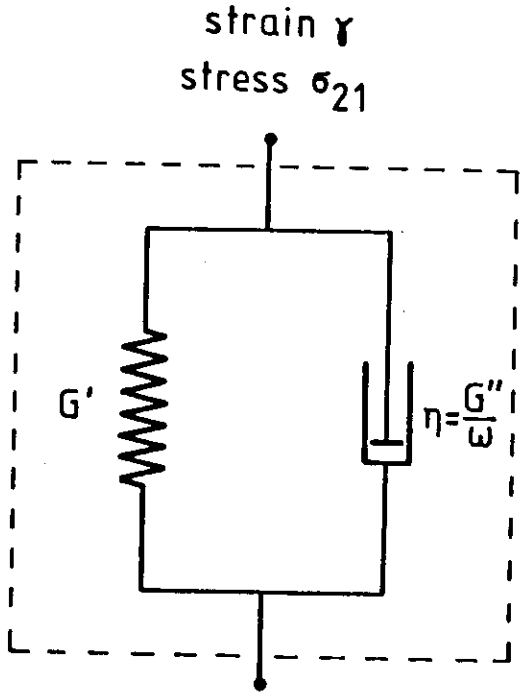

$$\sigma_{21} = G'\gamma + \eta\dot{\gamma} = G'\gamma + \frac{G''}{\omega}\dot{\gamma}$$

Fig.7: Representation of the response a viscoelastic fluid to oscillatory shear by a spring and dashpot arranged in parallel (G' and G" are frequency dependent).

The behaviour of long polymer chains dissolved in a viscous fluid (PIB macromolecules dissolved in oil in our case) can be understood as follows: at rest the molecules have a random coil like equilibrium conformation (left side of Fig.8). In a flow field the random coils immobilize part of the solvent giving rise to the observed viscosity increase with increasing polymer concentration.

If the equilibrium coil conformation remains undisturbed the solution would behave in a purely viscous manner.

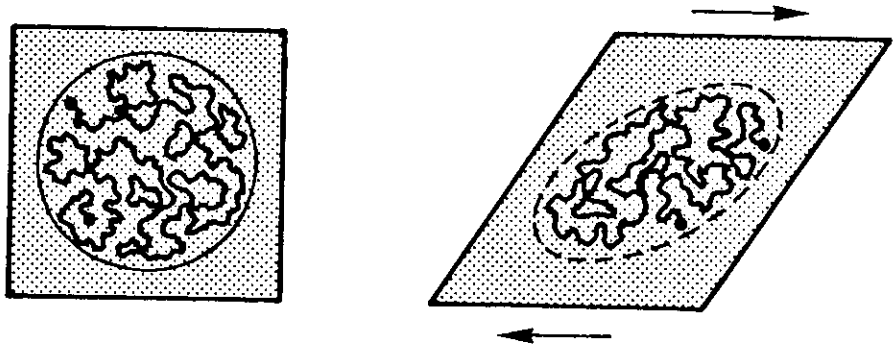

Fig.8: Equilibrium conformation (random coil) at rest and deformed state during flow of a macromolecule in solution (schematic).

In reality, during flow the molecule attains an ellipsoidal conformation (right side of Fig.8) and will partially be oriented parallel to the direction of flow. This deformation of the coil, however, is reversible. When the flow is stopped the molecule will re-establish its equilibrium conformation. This process takes some time and is governed by a characteristic retardation time τ. An estimate for the characteristic time is possible based on the moduli G' and G":

$$\tau = G'/\omega G'' \quad . \qquad (3)$$

It must also be mentioned that, if the solution is not kept under shape constraint after removal of the shear deformation, the re-attainment of the equilibrium random coil conformation will result in a reversed shear of the sample (Fig.9). The total recoverable strain γ_r, although difficult to measure on dilute solutions, may also be used as a direct measure of the elasticity of the sample besides the ratio G'/G".

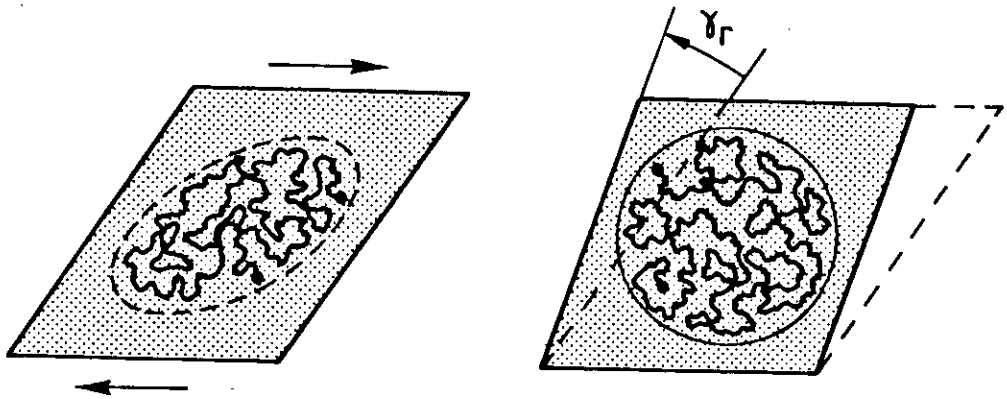

Fig.9: Recoverable shear strain of a viscoelastic solution after unloading due to the desorientation of deformed molecules.

Coming back to our measurements of the moduli G' and G" it is important to note that small amplitude oscillatory shear measures the viscoelasticity of the solution at small deviations from the equilibrium (coil-like) conformation of the dissolved PIB molecules.

As an example Figure 10 shows the measured dynamic moduli of a 16 000 ppm solution of ELASTOL in Petroleum. The pronounced viscoelasticity of the solution is evident from the fact that besides the loss modulus a distinct storage modulus can be measured. The ratio G'/G" increases with growing angular frequency.

The viscosity $|\eta^*|$ represented by the full symbols is calculated from the moduli according to

$$|\eta^*| = \frac{1}{\omega}\sqrt{G'^2 + G''^2} \quad . \tag{4}$$

This quantity is very close to the value of the viscosity in steady shear flow if ω is equal to the shear rate [4]. Thus, the decrease of $|\eta^*(\omega)|$ with increasing angular frequency reflects the non-

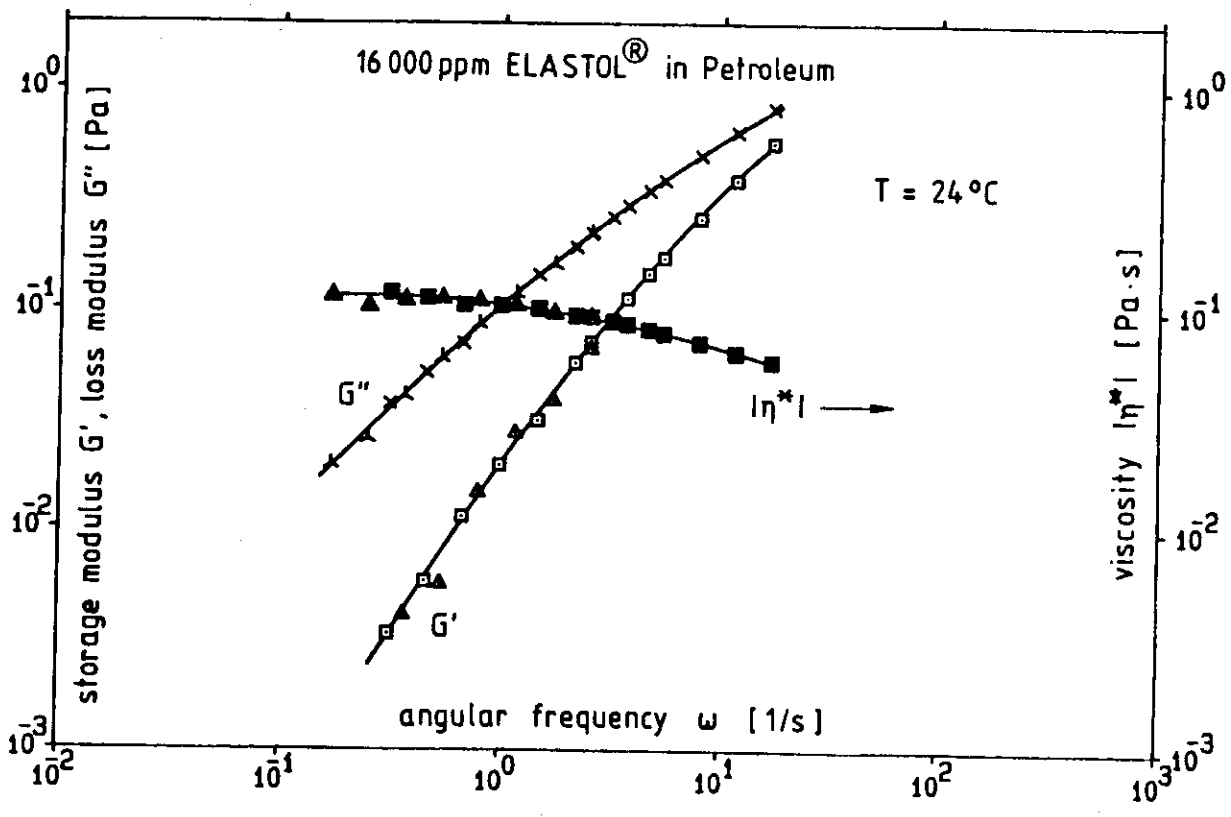

Fig.10: Storage and loss moduli (open symbols) and viscosity (full symbols) versus angular frequency of an ELASTOL solution in Petroleum at 16 000 ppm and 24 °C.

Newtonian behaviour of the solution, viz. the shear viscosity decreases with increasing shear rate. Again, this behaviour can be understood in terms of Fig.8. Deformed and partially oriented macromolecules give rise to a viscosity decrease depending on the shear rate.

Figure 11 shows the concentration dependence of the moduli in Dieselöl. The pure oil (full circles) is Newtonian and does not have a measurable storage modulus. In that case G" increases proportional to ω, the ratio G''/ω being equal to the viscosity η of the oil [3].

With increasing ELASTOL concentration the storage modulus grows stronger than the loss modulus. For $\omega = 1\ s^{-1}$ (0.13 Hz) a fourfold increase in concentration (4 000 ppm to 16 000 ppm) yields a G" growth of less than a factor of 20 whereas the storage modulus

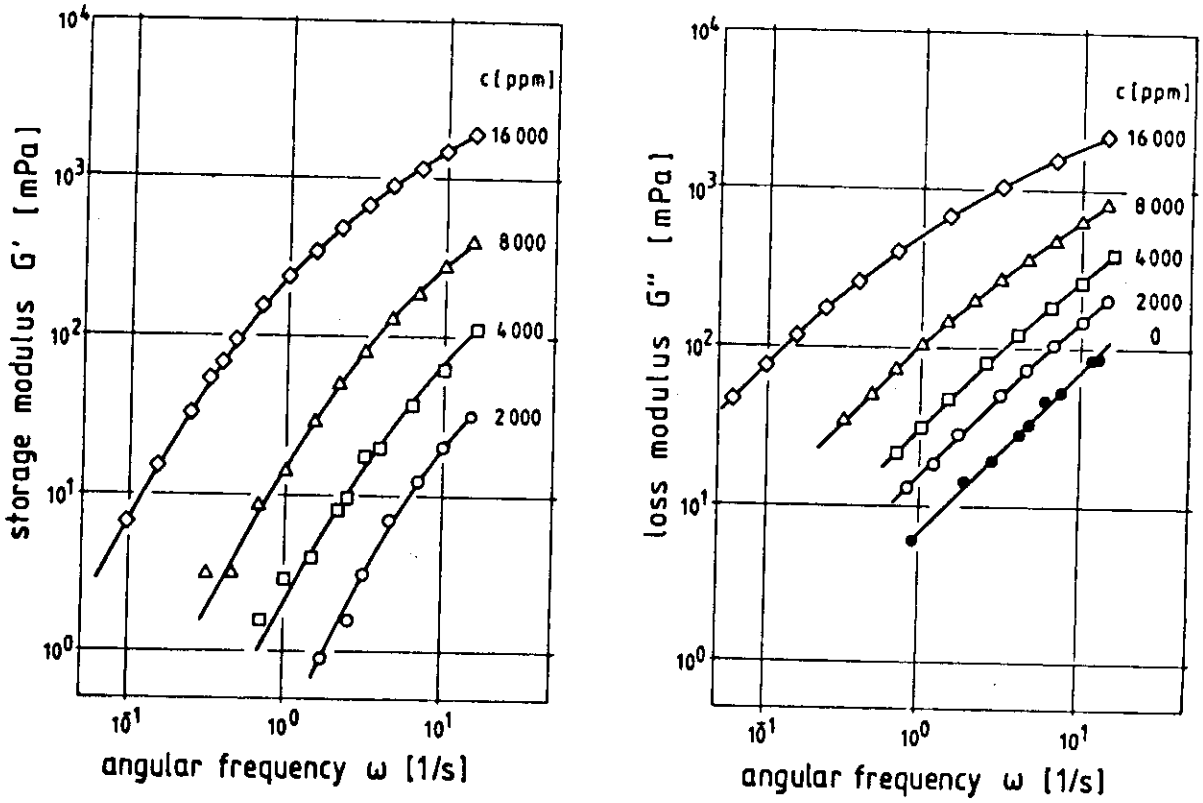

Fig.11: Storage modulus (left diagram) and loss modulus (right diagram) versus angular frequency of ELASTOL solutions in Dieselöl at various concentrations and 24 °C. The pure oil does not have a measurable storage modulus.

increases approximately 100-fold. As a result, the ratio G'/G" at a given frequency (cf. Table 3), taken as a quantitative measure of the viscoelasticity, increases considerably. It is also seen that in the same sequence the increase of G" is less than proportional to ω.

A comparison of the dynamic moduli for a constant ELASTOL concentration of 2 000 ppm in various oils of different viscosities is shown in Figure 12.

Table 3 gives a compilation of the moduli measured on various solutions. Here, the G' and G" are compared at a constant angular frequency of $\omega = 1.26\ s^{-1}$ (f = 0.2 Hz) and 24 °C. Besides the

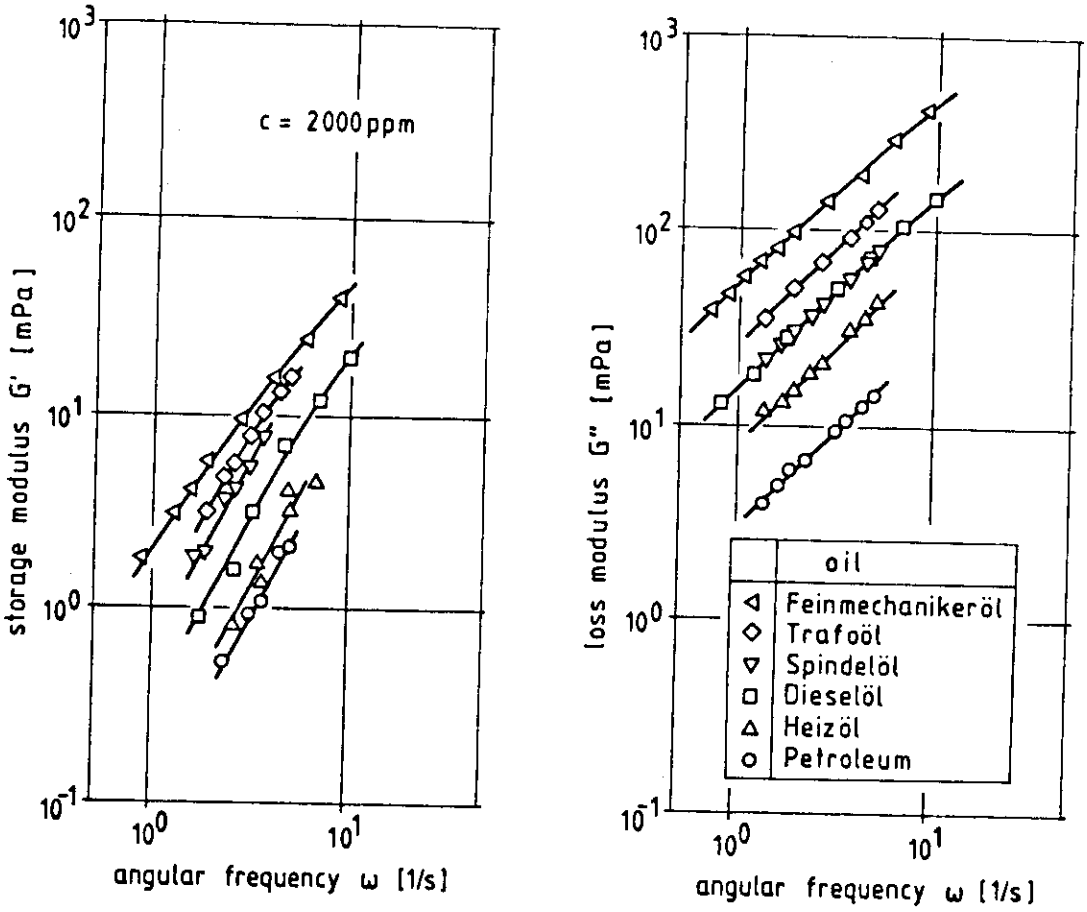

Fig.12: Storage modulus (left diagram) and loss modulus (right diagram) versus angular frequency for ELASTOL soulutions in various oils at a constant concentration of 2 000 ppm and 24 °C.

viscosity $|\eta^*|$ (Equ. (4)) and the ratio G'/G" this table also gives the characteristic relaxation time τ (Equ. (3)). For each oil both G'/G" and τ increase with growing concentration. The most pronounced changes are observed in the characteristic time.

Table 3: Dynamic moduli and viscoelastic properties of various solutions measured at $\omega = 1.26\ s^{-1}$ by means of small amplitude oscillatory shear.

	c [ppm]	G" [mPa]	G' [mPa]	$\lvert\eta^*\rvert$ [mPa·s]	G'/G"	τ [ms]
Petroleum	0	1.6	-	1.3	-	-
./.	8 000	23	1.6	18	0,07	55
./.	16 000	125	25.6	102	0.21	140
Heizöl	0	4.8	-	3.8	-	-
./.	4 000	12	0.35	8.8	0.03	23
./.	8 000	24	1.1	19	0.05	36
Dieselöl	0		-		-	-
./.	2 000	20	≈ 0.4	16	≈ 0,02	≈ 16
./.	4 000	39	3.2	31	0.08	65
./.	8 000	125	21.6	105	0.17	137
./.	16 000	590	290	523	0.49	390
Spindelöl	0	8.9	-	7.1	-	-
./.	2 000	18	0.65	14	0.04	29
./.	4 000	33	2.1	26	0.06	51
./.	8 000	85	12.6	68	0.15	118
Trafoöl	0	16	-	13	-	-
./.	2 000	34	2.3	27	0.07	54
Feinmechanikeröl	0	42	-	33	-	-
./.	2 000	67	3.0	53	0.04	35

4. Drawability (elongational viscosity) of ELASTOL solutions

One of the most striking effects of ELASTOL dissolved in oil is the dramatic increase in resistance to elongational flows. When the solution is stretched the PIB molecules are oriented which yields an elongational viscosity greater than three times the shear viscosity [5]. This behaviour is best demonstrated in the ductless siphon test [6] (Fig.13).

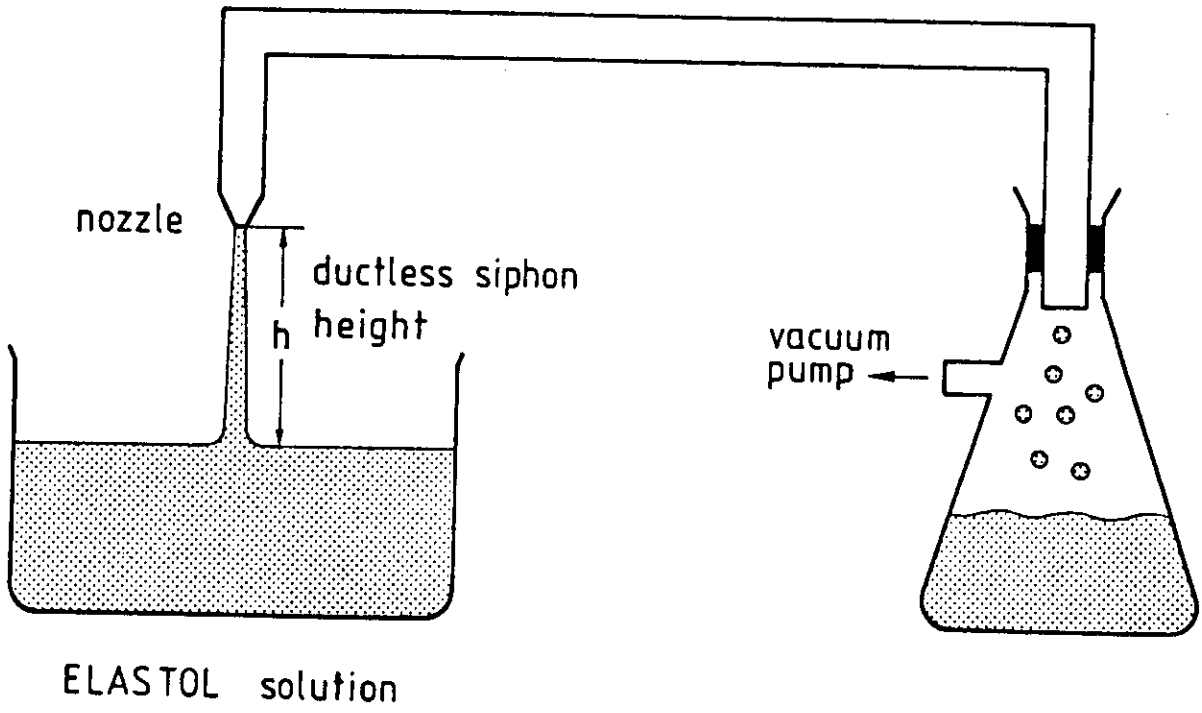

Fig.13: Schematic drawing of the ductless siphon test method. The ductless siphon height is gradually increased until break of the filament at h_{max}.

A pipe being connected to a vacuum pump carries a nozzle at its other end. The solution is contained in a beaker. When the nozzle is brought into contact with the meniscus of the solution the latter is sucked out of the beaker. The distance h between nozzle and solution meniscus is increased either by slowly lowering the container position or just due to the decreasing meniscus height for a fixed beaker position. The solution will still flow upward until at a maximum ductless siphon height h_{max} the filament breaks.

For an untreated oil, in general, the maximum ductless siphon height will be in the order of 1 mm. With ELASTOL h_{max} is much greater and may reach values of half a meter or more. This behaviour is of tremendous importance for the performance of collecting devices used for oil spill combat.

A photograph of the spinline in the ductless siphon test is shown in Fig.14 for a 4 000 ppm solution in Feinmechanikeröl (with red dye) and a nozzle diameter of 1 mm. The distance between the nozzle and the solution meniscus was 20 cm.

Fig.14: Ductless siphon test on a 4 000 ppm solution in Feinmechanikeröl. Nozzle diameter 1mm.

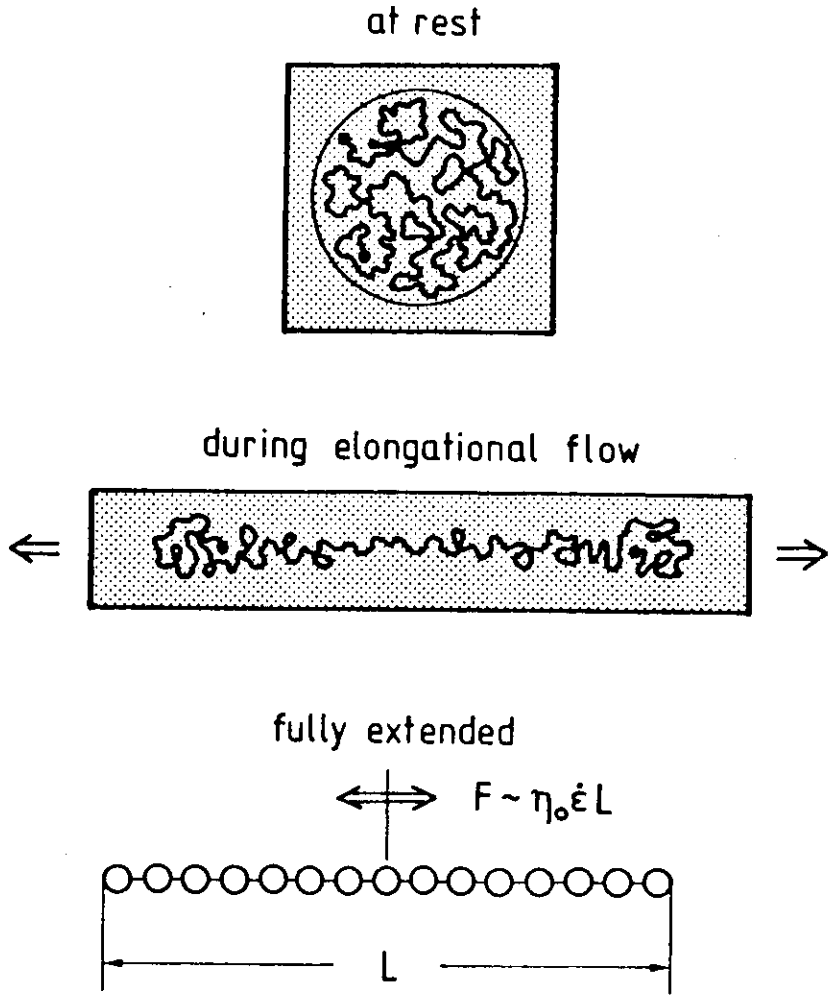

Fig.15: Stretching of the polymer chain when the solution is subjected to an elongational flow field (schematic).

The physical reason for the high elongational viscosity is schematically depicted in Fig.15. At rest the molecule has a coil like conformation, but in an extensional flow field, the molecule is stretched. The degree of stretching is dependent on the rate of strain of the solution and the duration of extensional flow. The sum of friction forces due to the surrounding solvent molecules has an opposite sign on both sides of the center of mass. Therefore, the extensional forces acting on the molecule are maximal in the middle of the chain and the orientation of chain segments parallel to the direction of strain is most pronounced in that region.

For the extreme case of a fully extended chain (bottom diagram in Fig.15) it is easy to show that the force F acting in the center of the molecule is proportional to the chain length L, the solvent viscosity η_0, and the strain rate $\dot{\varepsilon}$ [7]. The force F may even become higher than the chemical bond of the backbone. Under that condition the molecule will break [7].

It is obvious that in the case of long molecules the resistance to elongational flow is mainly governed by the force F that can be transmitted by each single molecule from one volume element to another and the concentration of dissolved macromolecules. In summary, we expect the elongational viscosity μ [5] of the solution

$$\text{elongational viscosity } \mu = \frac{\text{tensile force/cross section}}{\text{extension rate}} \qquad (5)$$

to increase with strain rate, solvent viscosity, and polymer concentration.

It should also be noted here that the stretched molecules store energy since the orientation process is fully reversible (chain rupture excluded). When the strain rate is set to zero the deformation of the molecule will decay with time until the coil conformation is re-established. Without shape constraint this process will cause a shrinkage (recoverable strain) of an elongated solution filament.

The measured ductless siphon heights h_{max} of Petroleum, Heizöl, and Spindelöl versus ELASTOL concentration are plotted in Figure 16. We observe a monotone increase of h_{max} with increasing powder concentration in Petroleum. For Heizöl and Spindelöl, however, h_{max} goes through a reproducible minimum. It appears that the concentration corresponding to the filament length minimum is shifted to smaller values when the oil viscosity is increased. Most probably this effect is not caused by a minimum in the true resistance of the filament to stretching but by problems in the nozzle flow due to the shear viscosity which increases with concentration.

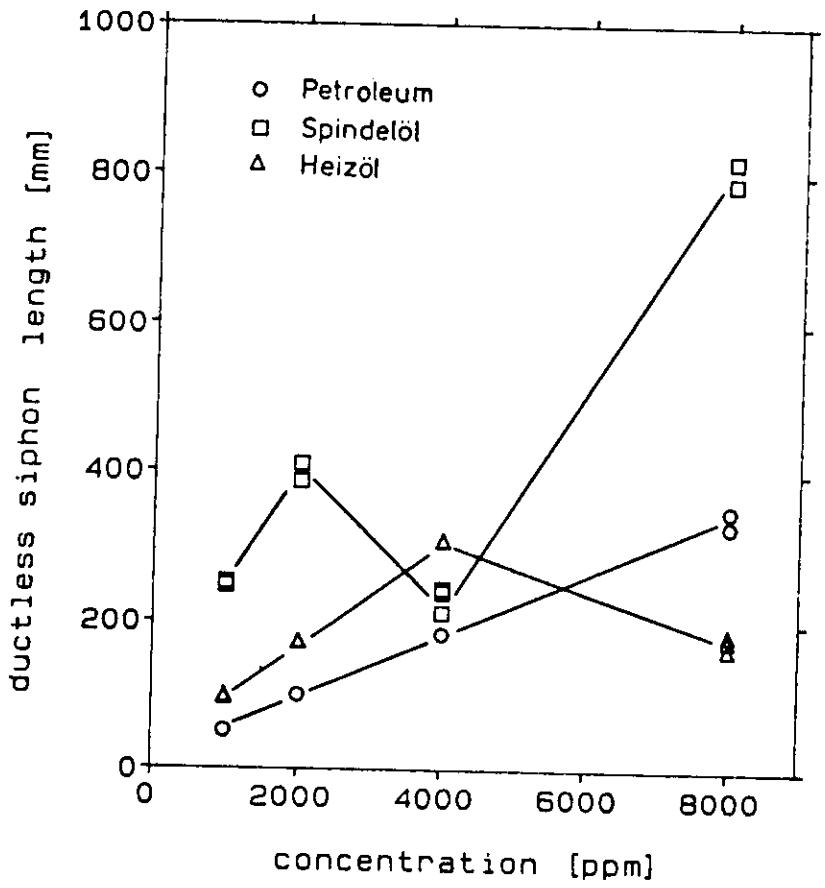

Fig.16: Maximum ductless siphon heights at room temperature for three oils versus ELASTOL concentration (nozzle diameter 1 mm).

Thus, for a direct comparison of the effect of ELASTOL on the drawability in various oil solutions one should restrict the measurements to concentrations below the minimum. In that range the behaviour may be approximated by the power law

$$h_{max} = K_{DS}\, c^{\alpha} \quad , \qquad (6)$$

the exponent α having values in the range of 0.75 to 0.95.

Table 4: Ductless siphon heights h_{max} at filament break for various oils and at an ELASTOL concentration of 2 000 ppm.

oil	η_0 [mPa·s]	h_{max} [mm]
Petroleum	1.42	100
Heizöl	3.8	187
Spindelöl	7.0	380
Trafoöl	13.0	471
Feinmechanikeröl	34.3	805

Table 4 gives a compilation of the measured h_{max} values in various oils for a constant ELASTOL concentration of 2 000 ppm. The maximum ductless siphon height strongly increases with increasing oil viscosity. Therefore, the higher the oil viscosity, the lower the concentration of ELASTOL required to obtain a given value of h_{max}.

As already mentioned , the drawability of ELASTOL solutions is an exclusively physical phenomenon. The application of chemical additives (for instance emulsion breakers) should have no influence on the ductless siphon heights. This was experimentally verified for Petroleum treated with 2 000 ppm ELASTOL and 100 ppm Separol AF 27 (BASF emulsion breaker). The same value of h_{max} as given in Table 4 for the pure Petroleum was observed.

The drawability increase due to ELASTOL is of great advantage in collecting oil floating on a water surface by means of a vacuum skimmer. A field test with crude oil (ERM) spread on water in a training basin gave the following results: In the case of untreated oil 90% water and only 10% oil were collected. After the application of
6 000 ppm ELASTOL powder 95% oil and only 5% water were collected [8]. Fig.17 shows that the oil film is pulled from the water surface without rupture and can easily be sucked by the vacuum skimmer over a distance of about 15 cm.

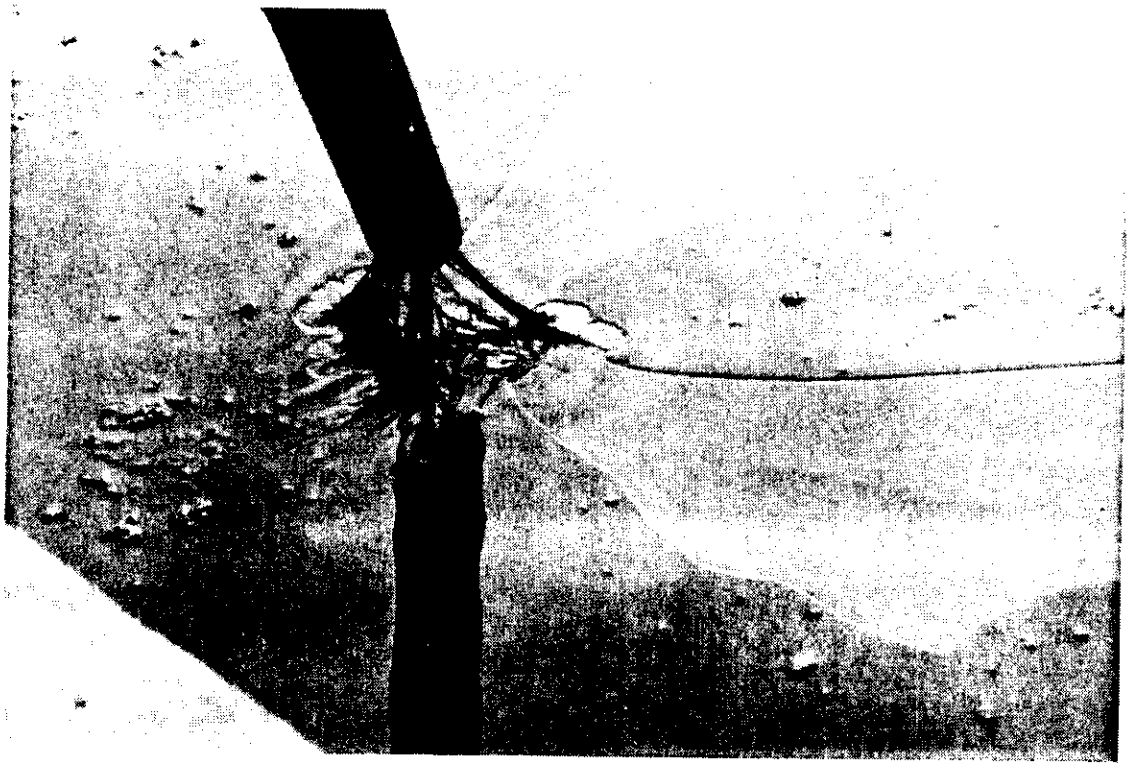

Fig.17: Example of the improved performance of a vacuum skimmer in collecting crude oil (ERM) from a water surface [8].

5. Consequences of ELASTOL on droplet formation

Fig.18 shows schematically the break up of an oil droplet into two smaller droplets due to an elongational flow field. Once a neck is formed the neck is elongated until break of the strap. The formation of smaller droplets continues until the rheological forces can no longer overcome the stabilizing effect of the interfacional tension.

With dissolved macromolecules, however, it is possible to prevent the formation of very small droplets [6]. Here, the limiting drop size is governed by the resistance of the strap to stretching. When the elongational viscosity in the neck is increased the break up process will come to an end at a bigger droplet size.

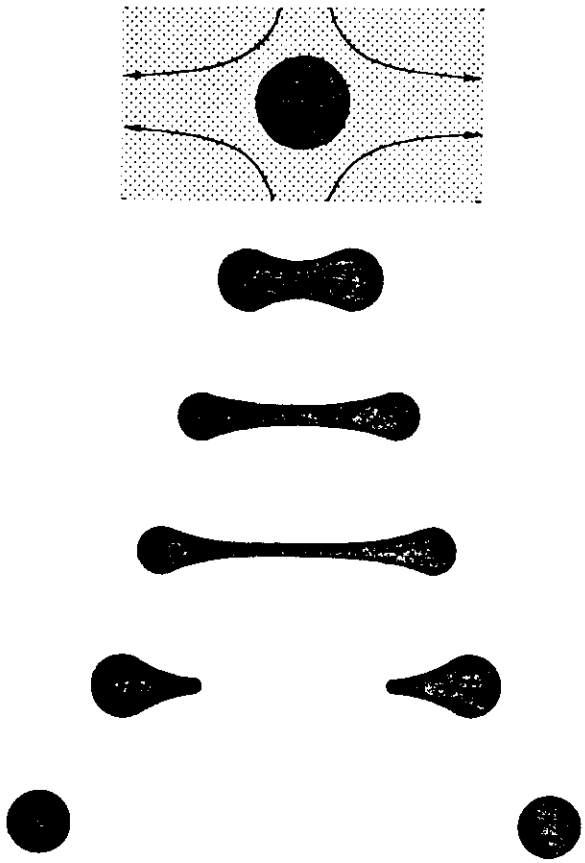

Fig.18: Formation of smaller droplets in an elongational flow field (schematic).

The consequence for oil/water mixtures is demonstrated by Fig.19. Two glass bottles were partially filled with water. In the right bottle pure Heizöl was used whereas in the left bottle the oil was treated with 10 000 ppm ELASTOL. The closed bottles were shaked by hand for a given time period. After a settling time of about 10 seconds we observe in the right bottle a milky emulsion of very small oil droplets in water. The water and oil phases are hardly separated. In the case of the ELASTOL treated oil (right) we get a coarse emulsion by shaking. The separation of water and oil is nearly complete after 10 seconds.

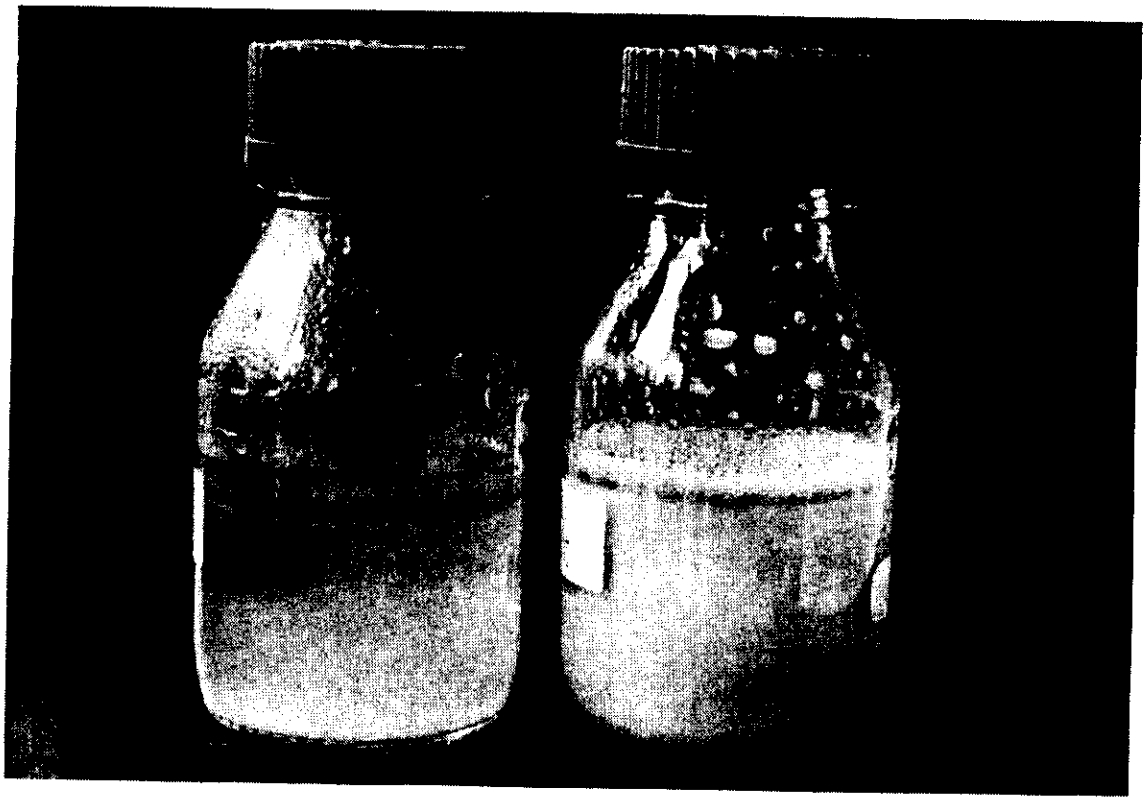

Fig.19: Dieselöl/water mixtures after shaking and a settling time of 10 seconds. Pure oil (right), oil treated with 10 000 ppm ELASTOL (left).

III. Dissolving behaviour of ELASTOL powder

a) General behaviour

The efficiency of ELASTOL in treating oil spills is strongly dependent on the dissolving speed of the powder after being spread onto oil layers floating on water. To simulate this situation on a laboratory scale a beaker of 150 mm diameter was partially filled with water. Oil was layered onto the water surface to a thickness of 5 mm. ELASTOL powder corresponding to 10 000 ppm of the weight of oil was "homogeneously" spread on the oil layer.

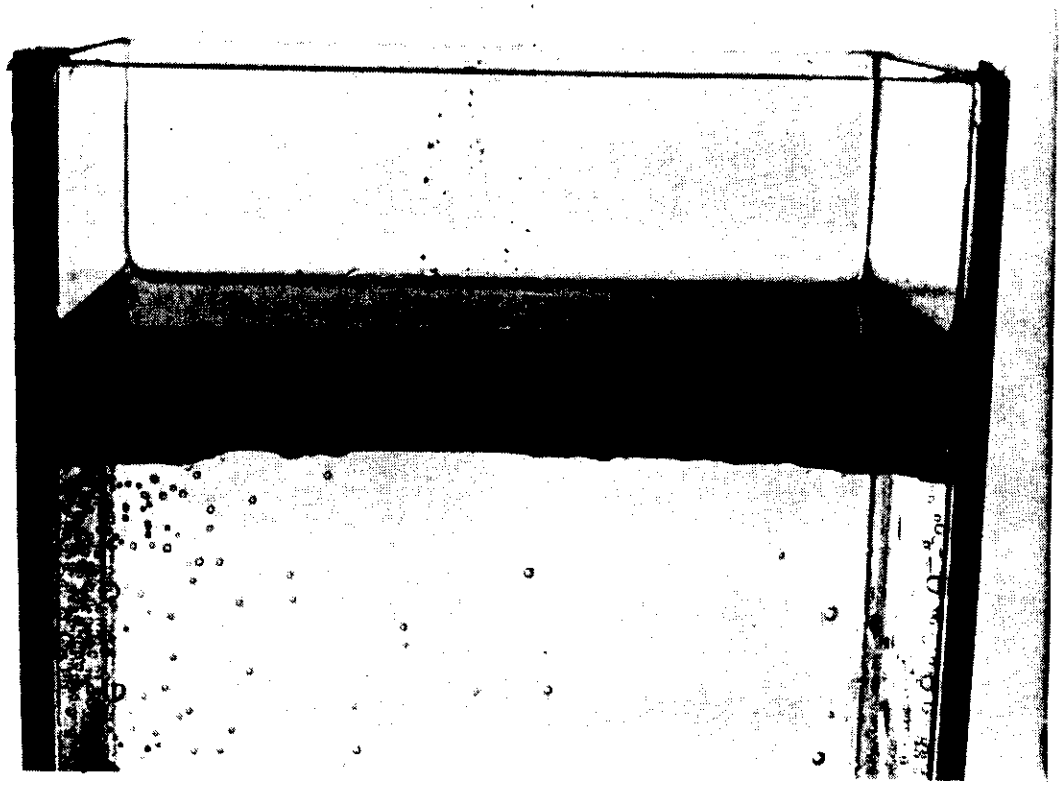

Fig.20: Side view of an oil layer floating on water. ELASTOL was spread on top of the oil and sedimented to the oil/water interface from where it dissolves.

After application, the powder rapidly sedimented to the water/oil interface (Fig.20). From there, the PIB component gradually dissolved in the oil phase, whereas the water-insoluble salt remained in particulate form at the interface. As a measure of the

effective solution concentration we determined the oil solution viscosity as a function of time. For this purpose small samples were withdrawn at different time intervals using a syringe. Precautions were taken not to collect undissolved PIB.

b) Solution viscosity with and without agitation

Figure 21 shows the solution viscosity versus logarithmic time as measured for Heizöl at a powder concentration of 10 000 ppm. In a first test series depicted by full circles the dissolving of ELASTOL

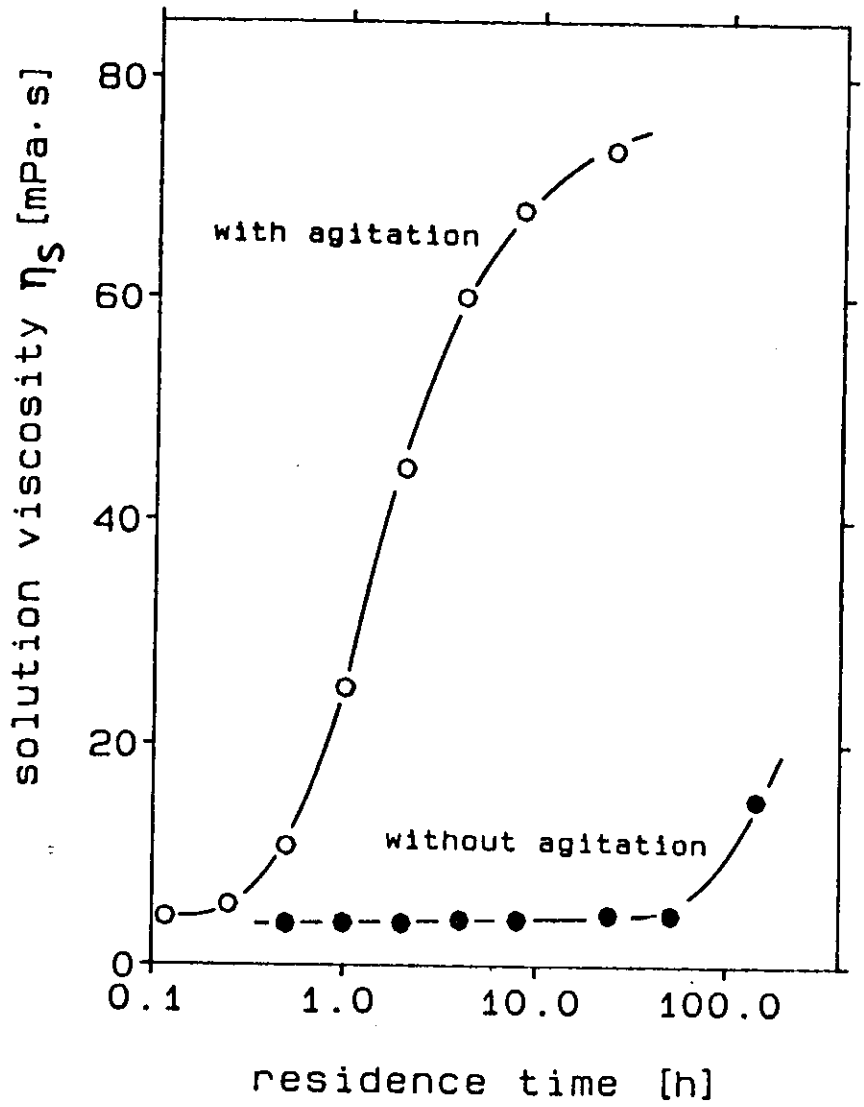

Fig.21: Relative solution viscosities of oil layers (5 mm thickness) floating on top of water versus time elapsed after application of ELASTOL by spraying (concentration 10 000 ppm related to the total weight of oil) with (open circles) and without (full circles) gentle stirring.

took place without any agitation. Obviously, in that case a significant increase of the solution viscosity is only observed at times greater than 100 hours.

In a second series of tests a gentle agitation was attained by stirring. A schematic drawing of the arrangement is shown in Figure 22. The rotary speed of the stirrer was 0.5 revolutions per second. As can be seen from Fig.21 the gentle agitation drastically increases the speed of dissolving (open circles). A significant increase in the oil solution viscosity was observed after only 0.5 hours.

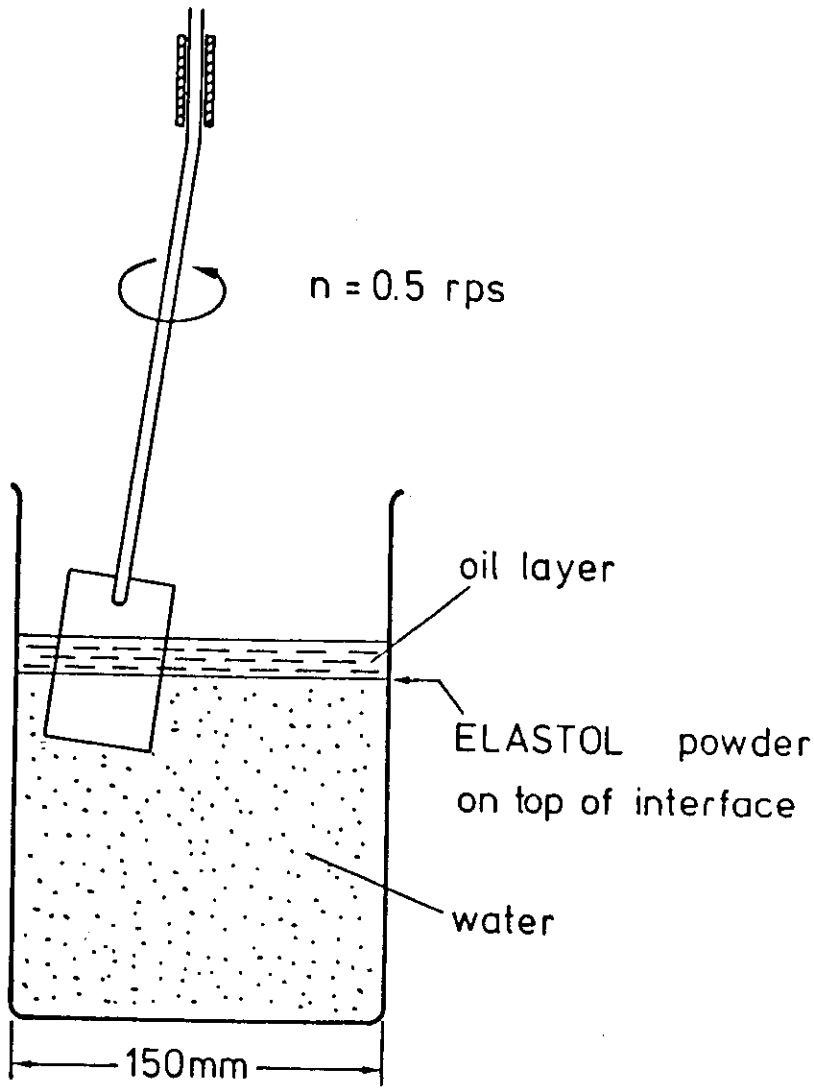

Fig.22: Experimental arrangement for the dissolving tests with stirring.

Similar dissolving tests with stirring were performed with various oils. The relative solution viscosities η_r (solution viscosity related to the oil viscosity) versus the oil viscosity η_0 are plotted in Figure 23. The data obtained by this method are more complex to interpret than those obtained by rolling (cf. Figs. 2 and 3). This is because partial evaporation of the oil has to be taken into account which is different for the various solvents. This explains why viscosities from the stirring experiment may be higher than those for solutions prepared by rolling in closed glass bottles.

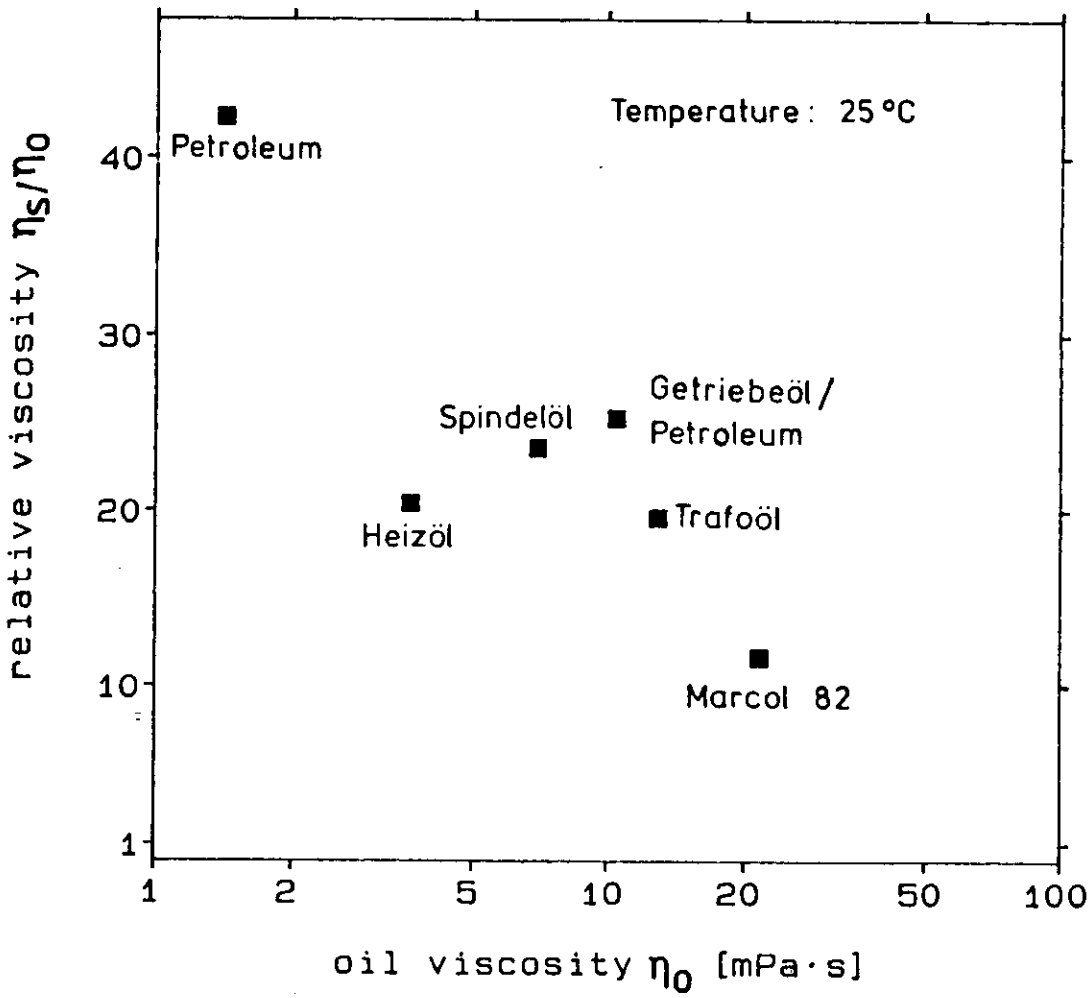

Fig.23: Relative viscosities of the various oil layers measured at the end of a 24 h stirring period. The initial powder concentration was 10 000 ppm related to the total weight of the oil on water.

c) Comparison of dissolving speeds

By comparing the viscosities determined for solutions prepared by rolling and the results obtained in the dissolving tests with gentle stirring (neglecting the influence of partial evaporation) we can evaluate the time necessary to dissolve an effective concentration of 2 000 ppm ELASTOL out of a total powder concentration of 10 000 ppm. The necessary times are plotted in Figure 24 as a function of the oil viscosities η_0 (double-log representation). The increasing dissolving time is approximately proportional to the oil viscosity.

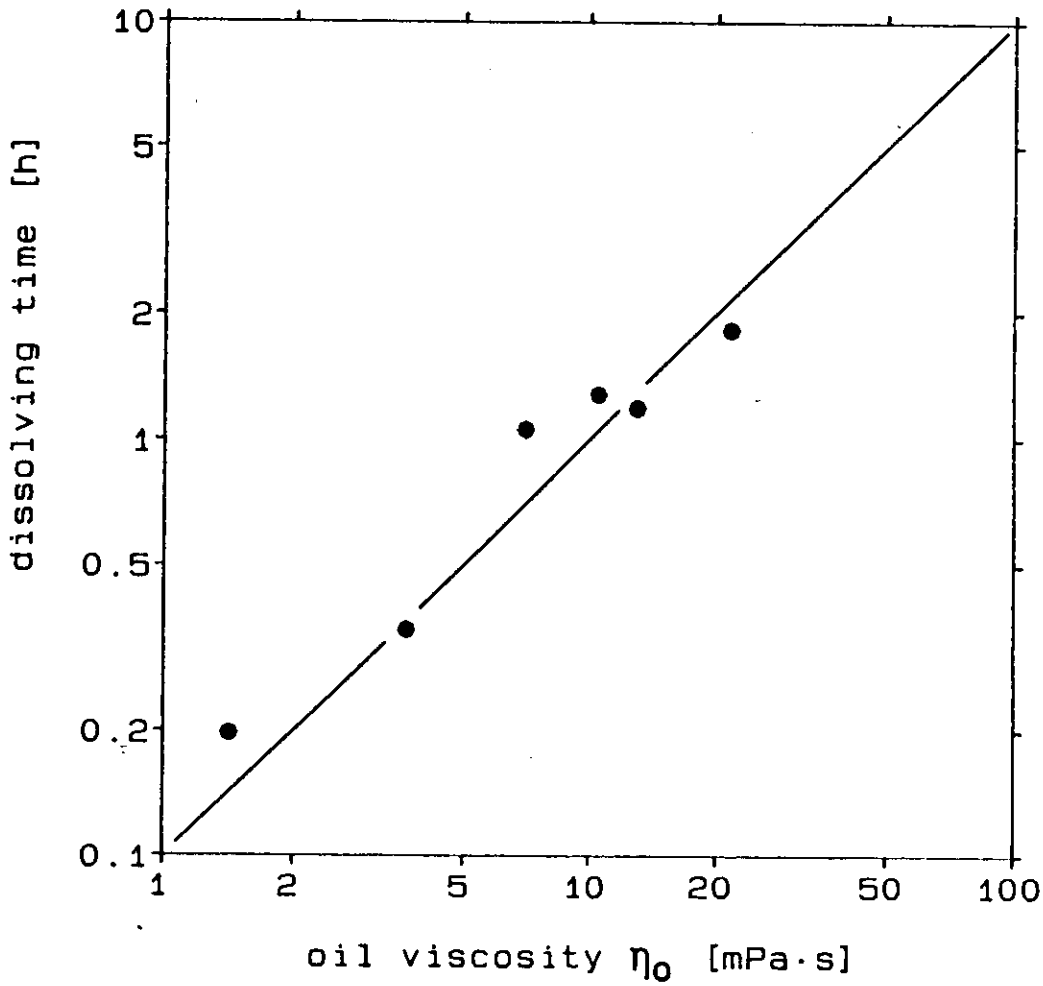

Fig.24: Dissolving time for 2 000 ppm ELASTOL out of an initial powder concentration of 10 000 ppm versus oil viscosity. The effect of partial evaporation during stirring is neglected here.

The data in Fig.24 can at least approximately be generalized for powder concentrations other than 10 000 ppm. Therefore, they can be used to estimate the time required to dissolve 20% of any quantity of ELASTOL powder.

In addition it is possible to estimate the effect of temperature on the dissolving time. For instance, if the viscosity of the oil increases by a factor x when the temperature is lowered by ΔT compared to room temperature, the necessary dissolving time of the powder will be longer by the same factor x.

IV. Water/crude oil emulsions

The formation of extremely stable water-in-crude oil emulsions, often called "chocolate mousse", is a major problem in combatting oil spills at sea. These emulsions are highly viscous and their water content can be as high as 90%. They are difficult to collect and even more difficult to dispose of. According to Bredie et al. [9] the formation of these mousses depends on the presence of both waxes and aspalthenes in the crude oil. These authors suggest that wax/asphaltenes crystals may stabilize small water droplets in the oil, leading to a dramatic increase in viscosity.

In order to produce "chocolate mousse" on a laboratory scale we performed experiments with various water-in-oil mixtures. In one series of tests different oil-water mixtures were treated with a shaker ("red devil") in closed bottles for 15 min. As expected the formation of a stable emulsion could not be observed for dewaxed and deasphaltenized oils like Trafoöl or Marcol 82. After a settling time of several minutes the water and oil phases separated. For the crude oils listed in Table 2, however, stable water-in-oil emulsions were easily produced by shaking. Even after a settling period of 24 hours no phase separation was observed.

The most stable "mousse" could be produced with Arabmed (η_0 = 18 mPa·s) for which a sudden rise in viscosity of the emulsion was observed with increasing water content. For a 70% water-in-oil emulsion a viscosity of 20 mPa·s was measured, whereas for 80% (90%) water content 6.1 (8.1) Pa·s were observed.

When the same experiments were repeated on Arabmed treated with 2 000 ppm ELASTOL the sudden rise in viscosity in going from 70% to 80% water content was reduced by at least a factor of 4. For both 80% and 90% water content viscosities of about 1.5 Pa·s were measured indicating that ELASTOL improves the pumpability of "chocolate mousse".

Fig.25: Stiff "chocolate mousse" obtained by shaking Arabmed with 90% water for 15 min in the red devil (right). Crude oil treated with 2 000 ppm ELASTOL (left).

Fig.25 demonstrates that without ELASTOL a stiff and stable emulsion with yield stress forms. When treated with ELASTOL, however, the Arabmed/water mixture was fluid even at very low shear stresses and had to be kept in a container. Also a tendency to phase separation between water and oil was evident.

a)

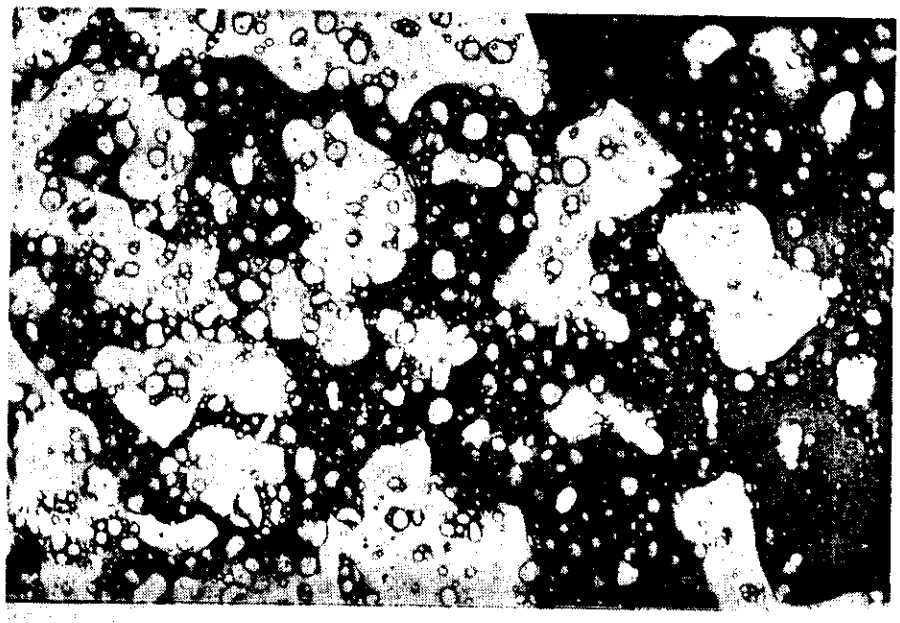

b)

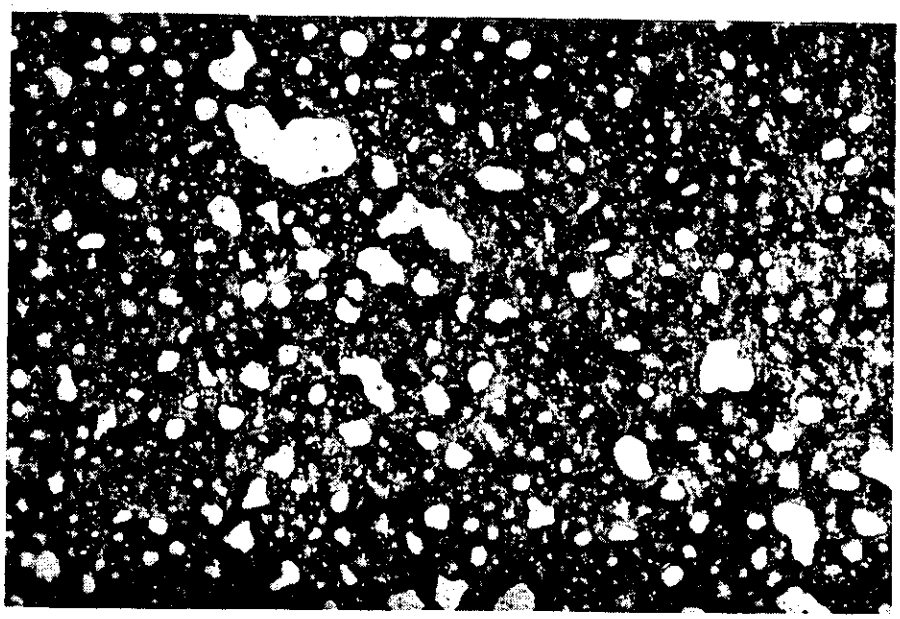

Fig.26: Light micrographs of 90% water-in-oil emulsions with Arabmed (magnification: 66 fold)
a) without ELASTOL b) with 2 000 ppm ELASTOL

Microscopic analysis of emulsions produced from Aramed and 90% water was carried out (Fig.26). Panel (a) shows the "chocolate mousse" formed with untreated Arabmed whereas Panel (b) demonstrates the effect of inclusion of 2 000 ppm ELASTOL. Both pictures illustrate the water-in-oil character of this emulsion, but for ELASTOL treated Arabmed the size of the water droplets is significantly smaller.

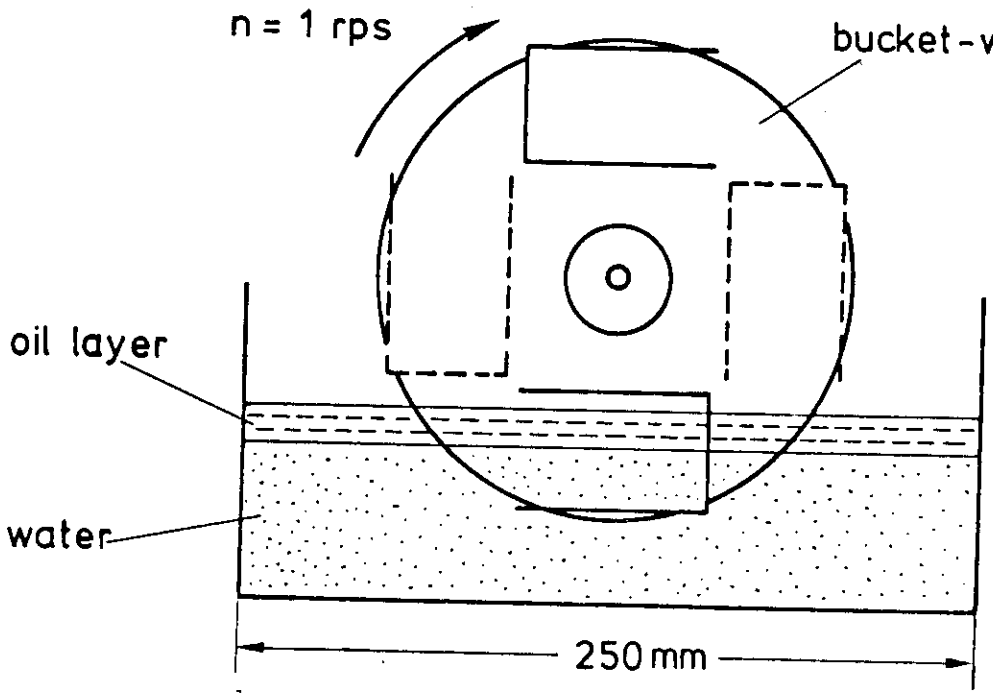

Fig.27: Experimental arrangement for the formation of "chocolate mousses" from crude oil layers floating on water.

In order to simulate the formation of "chocolate mousse" from crude oil layers floating on water more realistically, the apparatus schematically depicted in Fig.27 was used. Here the fluid was repeatedly picked up by a bucket-wheel and subsequently poured out onto the surface. In this arrangement the formation of stable emulsions was observed after stirring for less than 4 hours. After 4 hours the "chocolate mousse" formed with untreated Arabmed had a viscosity of 2 Pa·s.

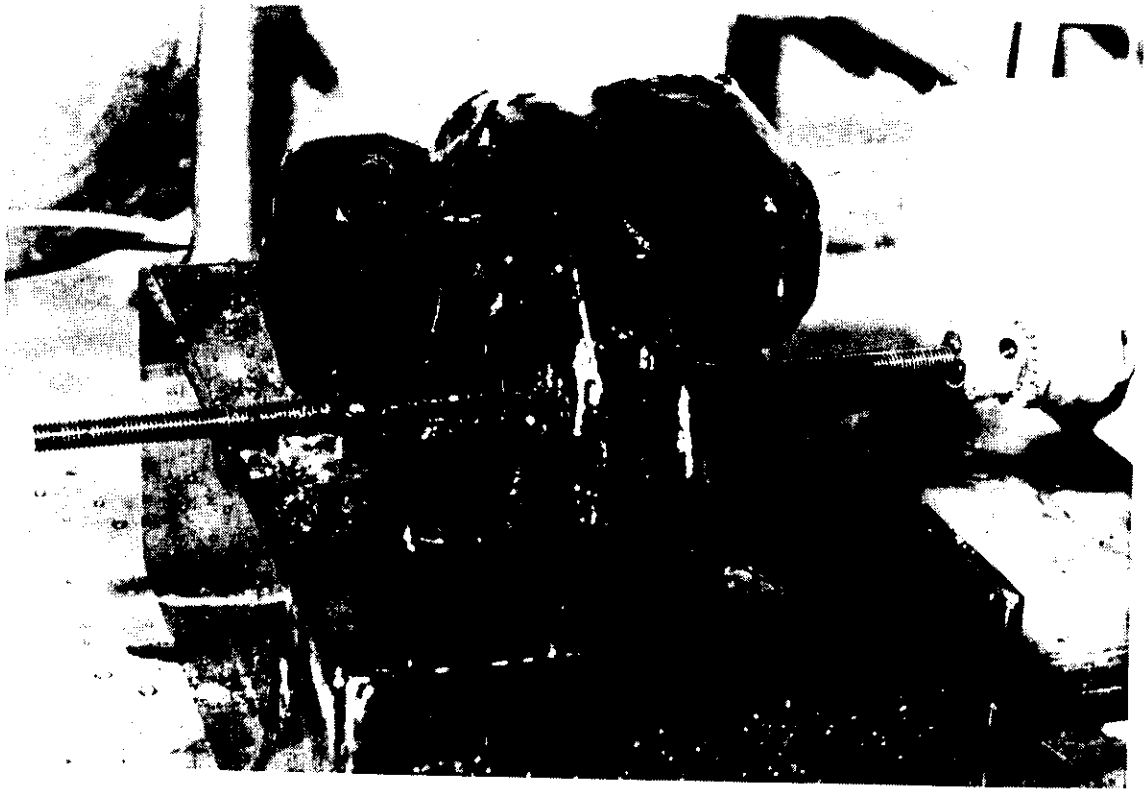

Fig.28: "Chocolate mousse" obtained with Arabmed in the bucket-wheel arrangement.

In addition, the bucket-wheel arrangement clearly shows the influence of evaporation. In Table 5 the emulsion viscosities measured after various stirring and evaporation periods are listed.

Table 5: Viscosities for "chocolate mousse" formed with Arabmed in the bucket-wheel arrangement (shear rate 2 s^{-1}).

stirring time [h]	residence time [h]	η_0 [Pa·s] untreated crude oil	η_0 [Pa·s] with 2 000 ppm ELASTOL
4	4	2.0	1.4
8	32	7.8	2.0
12	100	12.2	2.7
16	104	5.4*	

* Addition of 2 000 ppm ELASTOL to the "chocolate mousse" obtained from untreated Arabmed after 100 hours .

Stirring intervals of 4 hours and various rest periods have been applied. The first column gives the total stirring time and the second colum the total residence time of Arabmed in the bucket-wheel test. For the untreated crude oil the first stirring interval yields a "chocolate mousse" of 2 Pa•s. With increasing residence time due to evaporation the "mousse" viscosity increased up to 12.2 Pa•s (100 h).

When 2 000 ppm ELASTOL powder were spread on the mousse a drop in the emulsion viscosity to 5.4 Pa•s was observed after another stirring period of 4 hours (last line in Table 5). This means that the pumpability of the emulsion is improved and the advantage of elasticity is obtained by application of ELASTOL even after the formation of a stiff "mousse". When ELASTOL was spread on the oil layer at the beginning of the test, viz. before the formation of a "chocolate mousse", the effect of viscosity reduction was even more pronounced (fourth column).

Acknowledgement

The authors are indepted to W. Reuther, J. Steidel and Ch. Kaduk for performing the measurements and to M. Reuther for the support in preparing the diagrams.

References

[1] Bobra, M.A. and Kawamura, P.I. (Consultchem, Ottawa), Fingas, M. and Velicogna D. (Environtment Canada): LABORATORY AND THANK TEST EVALUATION OF ELASTOL T.M., Proceedings of the 10th artic and mirine oilspill program technical seminar, June 9-11, 1987, Edmonton, P. 223-241

[2] Huggins, M.L., J. Am. Chem. Soc. 64 (1942) 2716

[3] Ferry, J.D., VISCOELASTIC PROPERTIES OF POLYMERS, 2nd Ed., John Wiley, New York (1980)

[4] Cox, W.P. and Merz, E.H., J. Polym. Sci. 28 (1958) 619

[5] Jones, D.M., Walters, K. and Williams, P.R., Rheol. Acta 26 (1987) 20

[6] Chao, K.C., Child, C.A., Grens II, E.A., and Williams, M.C.: ANTI-MISTING ACTION OF POLYMERIC ASSITIVES IN JET FUELS, AICh. J. 30 (1984) 111

[7] Keller, A., J.A. Odell, Colloid & Polym. Sci 263 (1985) 189

[8] BASF film "Viscoelasticity - the new force in spill control and spill collection" (1986)

[9] Bridie, A.L. et. al., Wanders, Th.H., Zegfeld, W., van der Heijde, H.B., Marine Pollution Bulletin, Vol. 11, 1980, p. 343-348